Geophys. J. Int. (2002) **151,** 469–474

A study of gyroremanent magnetisation (GRM) and rotational remanent magnetisation (RRM) carried by greigite from lake sediments

S. Hu,[1,2] A. Stephenson[3] and E. Appel[2]

[1]*Nanjing Institute of Geography & Limnology, Chinese Academy of Sciences,* 73 *East Beijing Road, Nanjing* 210008, *P.R. China*
[2]*Institut für Geologie und Paläontologie, Universität Tübingen, Sigwartstr.* 10, 72076 *Tübingen, Germany. E-mail: erwin.appel@uni-tuebingen.de*
[3]*Department of Physics, University of Newcastle upon Tyne, Newcastle upon Tyne,* NE1 7RU, *UK*

Accepted 2002 May 14. Received 2002 May 7; in original form 2002 January 1

SUMMARY

Further studies of gyroremanent magnetisation (GRM) and rotational remanent magnetisation (RRM) have been conducted on lake sediments from the Zoigê Basin in the Eastern Tibetan Plateau, in which greigite is the main carrier of gyroremanent magnetisation. Greigite has the greatest effective gyrofield (B_g) of all magnetic minerals studied so far, being several hundred μT for a peak AF of 80 mT. This high B_g value has the potential to be used as an indicator for greigite. The GRM produced during static alternating field (AF) demagnetisation became close to its maximum at a peak AF of 150 mT. Attempts to extract the natural remanent magnetisation (NRM) by algebraic elimination of the GRM were unsuccessful above fields of about 30 mT because the GRM became much larger than the remaining NRM. The GRM of a crushed sample was much reduced because of the destruction of the sample's anisotropy, although as expected, both RRM and B_g were similar before and after crushing, thus demonstrating that RRM and B_g are independent of anisotropy. Measurement of the anisotropy of two samples from different depths showed that the deeper sample, which acquired the higher GRM, also had the higher anisotropy presumably as a result of greater sediment compaction. Study of anisotropy of GRM may help to elucidate the preferred alignment of greigite within the sample, which is difficult to ascertain by other means.

Key words: AF demagnetisation, anisotropy, greigite, GRM, lacustrine sediments, RRM.

INTRODUCTION

What are now known to be gyromagnetic effects in rocks have been reported for nearly three decades (Wilson & Lomax 1972; Stephenson 1980a,b, 1988, 1993; Dankers & Zijderveld 1981; Edwards 1982; Roperch & Taylor 1986; Snowball 1997a,b; Mahon & Stephenson 1997; Hu *et al.* 1998; Sagnotti & Winkler 1999). When certain rock samples are rotated in a slowly decaying alternating field (AF), a remanence, originally called a rotational remanent magnetisation (RRM), can be produced. Stephenson (1980a) explained it in terms of a gyromagnetic effect associated with a predominant sense of flip of moments inside the sample as it rotates in the field. Even during static three-axis AF demagnetisation, such gyromagnetic effects can produce a remanence in some anisotropic samples (Stephenson 1980b). It is appropriate to call this remanence gyroremanent magnetisation (GRM) but to keep the term RRM when specimen or field rotation is involved. This enables a distinction to be made between different methods of producing gyroremanences.

It is clear that both RRM and GRM is a nuisance in palaeomagnetic studies. They are unfortunately produced in precisely those rocks that are the most likely to be among the best types to be used for palaeomagnetic purposes (Stephenson 1993) since GRM is produced predominantly in single domain (SD) particles, which have high magnetic stability (Mahon & Stephenson 1997). Earlier RRM and GRM studies were focused on describing the phenomenon and establishing a general theory of this new remanence (Wilson & Lomax 1972; Stephenson 1980a,b, 1981, 1988, 1993; Smith & Merrill 1980; Edwards 1982). Later, increasing efforts were made to correct the abnormal remanence directions caused by GRM after AF demagnetisation (Dankers & Zijderveld 1981; Roperch & Taylor 1986; Stephenson 1993; Hu *et al.* 1998). Dankers & Zijderveld (1981) first proposed an empirical method to correct GRM-induced abnormal remanence directions, while Stephenson (1993) gave a theoretical confirmation of their method. Most studies, until recently, have involved magnetite-bearing samples but recently it has become apparent that greigite shows an even greater gyromagnetic effect (Snowball 1997a,b; Hu *et al.* 1998; Stephenson & Snowball 2001). It is worth to mention that great efforts have been made to study the magnetic properties of greigite (e.g. Hoffmann 1992; Hallam & Maher 1994; Sagnotti & Winkler 1999; Dekkers & Schoonen 1996; Roberts *et al.* 1996; Torri *et al.* 1996). Much of the natural sedimentary greigite data display single-domain-like magnetic properties (Snowball 1991; Roberts 1995). The observation of dominantly SD-like properties are probably related to the lower saturation magnetisation of greigite with respect to magnetite and, therefore, the broader range of grain sizes in which greigite can retain SD-like properties. However, the fundamental magnetic properties of greigite are still not totally understood. Identification of greigite by magnetic and geochemical analyses is still somewhat difficult in practice. Therefore, measurement of B_g, which is rapid, may prove useful in this respect since greigite seems to have the highest B_g of all other magnetic minerals reported so far. The advantages of using B_g to identify greigite are summarized by Snowball (1997b): the method is based solely on remanence parameters (and is therefore unaffected by diamagnetic and paramagnetic components); and it is possible to detect low concentrations of greigite without elaborate sample separation. In this paper, we report measurements of RRM, GRM and B_g for greigite-bearing samples and attempts to correct for GRM-induced abnormal remanence directions during static AF demagnetisation. The samples studied in this paper are lake sediments from the Zoigê Basin, eastern Tibetan Plateau, China. Related information, such as the geological setting, sampling, rock magnetism, and general GRM properties, have been described in a previous paper (Hu *et al.* 1998), and environmental magnetic results from this ancient lake may be obtained from Hu *et al.* (1999). In our previous GRM study, single-domain greigite is identified as the main carrier of GRM.

METHODS

Most GRM experiments reported in this paper were done in the Palaeomagnetic Laboratory, Institut für Geologie und Paläontologie, Universität Tübingen, Germany. A SQUID magnetometer with an attached automatic degausser system (2G Enterprises) was used for the GRM study in Tübingen, and the working method was described by Hu *et al.* (1998). All experiments on RRM, together with part of the GRM anisotropy study, were done in the Department of Physics, University of Newcastle upon Tyne, UK. Instrumentation used in Newcastle for RRM and GRM studies were described by Stephenson (1980a,b) and by Stephenson & Molyneux (1987).

B_g VALUES

The effective biasing field (gyrofield), B_g, was defined as 'the steady field which, if applied along the high speed rotation axis of a spinning sample in the presence of a slowly reducing AF from 80 mT peak (applied at 90° to the spin axis), would give an anhysteretic remanent magnetisation (ARM) equal in magnitude to the RRM' (Potter & Stephenson 1986). B_g is expressed as:

$$B_g = B_a^* \mathrm{RRM}/\mathrm{ARM}$$

where B_a is the steady bias field used to produce ARM.

B_g values were obtained from 10 samples. The RRM and ARM (70 μT bias field) were measured for the 10 samples using a peak AF of 80 mT and a rotation speed of 95 rps in a rotational magnetizer (Stephenson & Molyneux 1987). RRMs are between about 1 and 10 times stronger than ARM (Table 1). B_g values thus range between 77 and 734 μT. The maximum B_g (at 80 mT) for magnetite measured to date is 300 μT for an artificial powder of grain size 0.2 to 0.8 μm (Potter & Stephenson 1986) and thus greigite within the sediments of the Zoigê Basin is capable of higher B_g values than magnetite. Snowball (1997b) reported B_g values of around 84–137 μT for SD greigite, but only about 3.6–14 μT for SD magnetite at peak AF of 100 mT using a rotation speed of 5 rps. Under the same conditions as used here (80 mT and 95 rps), some of Snowball's (1997b) samples gave B_g values of about 1100 μT (Stephenson & Snowball 2001), about an order of magnitude higher than that found for typical magnetite-bearing rocks so the high values in the Zoigê Basin samples are in line with those obtained previously for greigite-bearing samples.

Table 1. RRM, ARM and B_g values for 10 greigite-bearing samples.[1]

Sample	RRM (mA m^{-1})	ARM (mA m^{-1})	Bg (μT)
T3108	2.3	2.1	77
T3164	531	62	597
T3170	461	70	461
T3182	125	14.3	613
T3198	3.3	2.1	110
T3318	283	27	734
T3422	10	1.6	440
T3446	78	8.9	614
T3496	218	24.3	628
T3607	924	119	546

[1]For a rotation speed of 95 rps, a peak AF of 80 mT and a steady field (for producing ARM) of 70 μT.

A few samples (T3108, T3198, and T3422) with low RRM also have the lowest values of B_g. A possible explanation for this is that there may be a higher proportion of magnetite coexisting with greigite within these 3 samples (Hu *et al.* 1998; Hu 1998). For the same overall magnetic mineral content this would account for both the lower RRM and the lower B_g.

CORRECTION FOR THE EFFECT OF GRM ON THE NRM DIRECTION

Dankers & Zijderveld (1981) proposed a method (determined empirically) to remove GRM produced by static three-axis AF demagnetisation. Since no GRM acquisition is expected along the demagnetisation axis, measurements of all three components after each demagnetisation step in the *x*-, *y*-, *z*-directions provide results that are not affected by GRM. Stephenson (1993) showed theoretically that this method of treating the experimental results to reveal the NRM vector algebraically eliminates GRM. Hu *et al.* (1998) tried in the same way to extract NRM data in the presence of GRM, but poor results were obtained. Three possibilities were proposed to explain the failure of the GRM correction: (1) the acquired GRM was much stronger than the NRM; (2) tumbling demagnetisation step, suggested by Stephenson (1993), was not used between each static demagnetisation (such method has the effect of randomizing the gyromagnetically generated moments because of simultaneous rotation about several axes); (3) perhaps a small GRM component might even be produced along the AF demagnetisation direction.

In this paper we also present results of a correction test on the sample T3470. The variation of remanence intensity versus AF before and after correction is shown on Fig. 1. Between 0 and 20 mT, the sample was treated with static AF demagnetisation in turn along the *z*, *y*, and *x* axes. After the AFs were applied along 3 axes, the remanence was measured. This is a standard (but not a very good) way to do static AF demagnetisation, because any GRM produced by the last AF application will be added vectorially to the remaining NRM and thus an incorrect apparent NRM direction will be obtained.

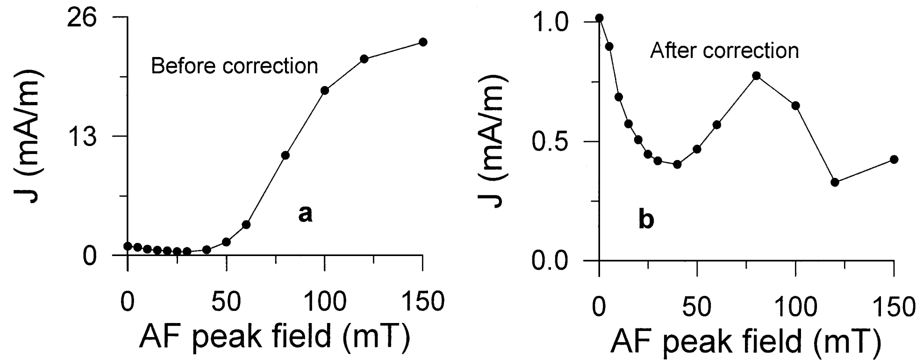

Figure 1. GRM correction test on sample T3470. (a) A GRM was acquired at higher fields during 3-axis static AF demagnetization; (b) intensity variation versus AF (after GRM correction using the Dankers & Zijderveld 1981 method). See detailed explanation in text.

It is clear that no significant GRM was acquired below 20 mT since the NRM decreases smoothly. Above 20 mT, the method of Dankers & Zijderveld (1981) was used to extract the characteristic NRM. The sample was demagnetised in the same way, but the complete remanence was measured after demagnetisation along each axis. This procedure was repeated up to 150 mT. Following Hu *et al.* (1998), the remanence components measured after demagnetisation along the last step (the x axis) for each peak field were used to calculate the normalised intensity decay curve during demagnetisation (marked 'before correction' in Fig. 1a). The three diagonal components were used to calculate the intensity for the corrected results (marked as 'after correction' in Fig. 1b).

The results of Fig. 1(a) show that the GRM acquired at higher fields is strong (23.2 mA m^{-1} at 150 mT). The NRM of sample T3470 is, however, only 1.02 mA m^{-1} and thus the GRM is about 20 times stronger than the NRM. In Fig. 1(b), the intensity falls initially after correction but then increases above 50 mT, showing that the GRM is not being removed. The data after treatment at 150 mT are shown in Table 2 and behave in accordance with the Stephenson model (Stephenson 1993). All three diagonal components are small, which means that no (or little) GRM was produced along the AF demagnetisation direction, while the pairs of non-diagonal components in each column are nearly equal and opposite. All of these observations are as expected. The x and y diagonal components are -0.37 and -0.20 mA m^{-1}, respectively. In their previous steps, they were -14.43 and -20.31. This means that the AF treatment demagnetised the GRM component along the field direction to about 1 or 2 per cent. However, since the initial remanence is only 1.02 mA m^{-1} these residual parallel GRM components are not small compared to the remaining NRM and so the GRM correction fails at high fields. This is a general characteristic for any material since the GRM inevitably increases with field while at the same time the remaining NRM is gradually decreasing to zero. The effect, however, is worse for greigite because of its propensity for acquiring GRM. The same correction tests were also conducted on the samples T1512, T1786, T3156 and T3406, with the similar results.

Table 2. x, y and z remanence components after each AF demagnetization step.

	x (mA m^{-1})	y (mA m^{-1})	z (mA m^{-1})
AF along x axis (last step)	−0.37	21.57	8.65
AF along y axis (second)	−14.43	−0.20	−8.41
AF along z axis (first)	15.61	−20.31	0.06

GRM ACQUIRED BY A POWDERED SAMPLE

Sample T3184 was subjected to normal stepwise static AF demagnetisation up to 150 mT (The last axis used every time was the x axis). It was the first time that the sample T3184 was subjected to static AF demagnetisation treatment. From Fig. 2(a), it can be seen that about 66 per cent of the NRM were removed at 60 mT (demag 1).

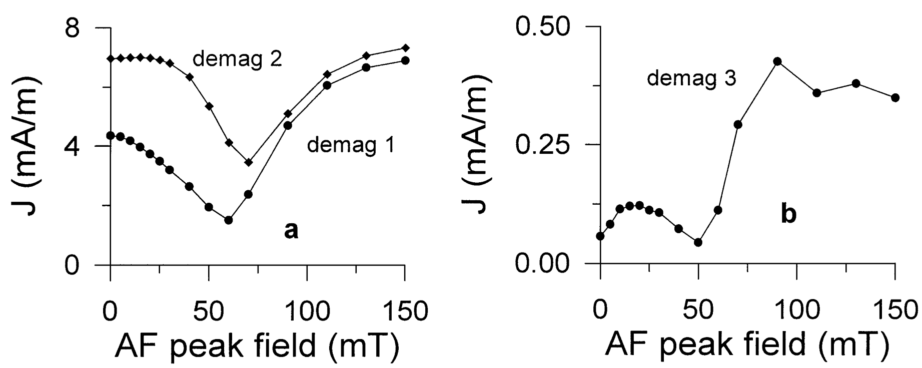

Figure 2. Stepwise AF demagnetization for sample T3184. (a) Stepwise 3-axis AF demagnetization of the NRM (demag 1). The sample was then AF demagnetized again using the same procedure (demag 2). In the second AF demagnetization, GRM was stable up to 25 mT. GRM acquisition above 60 mT is similar in the two cases. (b) Stepwise 3-axis AF demagnetization after the sample was crushed and stirred (demag 3).

Above 60 mT, it is clear that a GRM was acquired (6.90 mA m^{-1} at 150 mT compared with an NRM of 4.36 mA m^{-1}).

In the second step, the sample was treated with static stepwise AF demagnetisation again with the sample in the same orientation (Fig. 2a, 'demag 2'). It can be seen that the GRM was not removed at all below 25 mT, while upto a field of 70 mT, the GRM was reduced to values 20 per cent below the NRM intensity before any AF application (4.36 mT). This shows that the GRM acquired in peak AF of 150 mT is magnetically harder than the NRM. The GRM intensity was reduced to half at 70 mT in demag 2 and was 7.33 mA m^{-1} at 150 mT, nearly the same as in demag 1.

The sample was then crushed and ground into a powder. Since lake sediment is fairly friable, it was easily crushed and ground using a pestle and mortar. The powder was stirred in order to attempt to destroy any anisotropy due to particle alignment. During this procedure, no liquid was used. We will confirm later that no change of magnetic mineralogy resulted from such treatment. Before crushing, the anisotropy of magnetic susceptibility (AMS) was measured. P ($\kappa_{max}/\kappa_{min}$) and L ($\kappa_{max}/\kappa_{int}$) for this sample were 1.027 and 1.002, respectively. The declination/inclination for κ_{max}, κ_{int}, κ_{min}, are 216/6, 125/7 and 348/81, respectively (declinations are arbitrary since the core was obtained by the rotating drilling process). It should be stressed that a paramagnetic contribution is important for sediments in this core, as confirmed in a previous investigation (Hu 1998). After crushing and stirring, the preferential alignment of magnetic particles should be destroyed. The powder was then put into the sample holder again, taking care to minimise the pressure in order to avoid introducing anisotropy. Stepwise static AF demagnetisation was applied to the powder as before (Fig. 2b, 'demag 3'). The remanence was greatly reduced from 7.33 mA m^{-1} to 0.057 mA m^{-1} after crushing, grinding and stirring. Meanwhile, the GRM acquired at high field is only about 0.37 mA m^{-1}, presumably due to the much reduced anisotropy (it is a factor of 20 less than that obtained before crushing as shown in Fig. 2a).

Sample T1512 and T3604 were chosen for a further crushing test. GRM, RRM and ARM were measured before and after the samples were crushed (Table 3). A GRM was produced at 80 mT with demagnetisation successively along the z, y, x axes. An RRM was imparted in peak AF of 80 mT, and the sample was rotated at 95 rps about the z axis (i.e. normal to the bedding plane). An ARM was also acquired along the z axis in the same AF, with a bias field of 70 μT. After weighing, the samples were crushed, ground and stirred. Both samples were weighed again after crushing so that small losses of sediment could be allowed for, i.e. the remanences before crushing were normalized to the weight after crushing. The data are shown in Table 3. The GRM of both samples decreased markedly after crushing, as expected, because the anisotropy was destroyed.

After crushing, B_g decreased slightly for sample T1512, but it remained about the same for sample T3604. This is not surprising because crushing, grinding and stirring did not cause a change in the magnetic mineralogy.

The RRM and ARM of both crushed samples increased by around 10 per cent after crushing (Table 3). This is probably because the acquisition of these remanences in the uncrushed (anisotropic) sample was along the z axis (i.e. normal to the bedding plane) where the remanence is smallest. After crushing, the sample becomes almost isotropic and so the RRM and ARM increased (i.e. the sum of the principal remanence axes is constant before and after crushing, but since the z axis is the smallest before crushing, an increase is observed after crushing when all the axes become equal).

GRM ACQUISITION DIFFERENCES

Hu *et al.* (1998) reported that in these sediments there are two types of samples based on GRM acquisition behaviour. In the first type, GRM was of the same order as the NRM (most samples belong to this type), while GRM was much stronger than NRM in the other type (see Fig. 7, and 'GRM samples distribution' in Fig. 1, Hu *et al.* 1998). In both types of samples the magnetic properties were the same, but most samples with GRM larger than NRM were distributed near the bottom of the core (see Fig. 1, Hu *et al.* 1998). An obvious explanation for this observation is that, since GRM is proportional to anisotropy for a given mineralogy, the higher GRM of the lower samples is due to a higher anisotropy because of increased compaction at depth.

To test this idea, two more samples were examined. The NRM of sample T1786 is 4.82 mA m^{-1}, and its GRM acquired at the peak AF of 150 mT (last AF along the x axis) is 3.03 mA m^{-1} and is thus of similar magnitude (Table 4). Another sample T3470 is from a greater depth in the core, and has an NRM of 1.02 mA m^{-1}, and a much larger GRM of 23.2 mA m^{-1} (at a peak AF of 150 mT). RRM and ARM were therefore measured for these two samples under the same conditions as for samples T1512 and T3604 to test the hypothesis that anisotropy increases with depth. Both samples acquired different amounts of GRM (different by more than a factor of 7), but they have similar B_g values. This supports the previous conclusion that the two types of samples have the same magnetic mineralogy. GRM, as expected, is much lower than RRM, being about 0.9 per cent and 5 per cent for the weak and strong samples, respectively.

To make sure that different GRM values were not just simply due to different AF orientations relative to the anisotropy axes, 6 different orientations x, y, z, and x'', y'', z'' were used (for details, see Fig. 4 in Stephenson 1993). From such measurements the actual GRM anisotropy ellipsoid can be calculated. The results are shown in Table 5 where both, the orientation of the ellipsoid and the difference in GRM values (C1, C2, C3) between the principal axes (x', y' and z') are listed.

It is clear from Table 5 that the intensity differences between x' and y' in both samples are relatively small compared with the differences between z' and either x' or y'. This indicates that both samples have an oblate anisotropy ellipsoid. However, the differences

Table 3. GRM, RRM, ARM and B_g values before and after crushing.

	T1512		T3604	
	Before	After	Before	After
GRM (mA m^{-1})	0.55	0.2	144	2.1
RRM (mA m^{-1})	55.6	63.9	506.5	576.2
ARM (mA m^{-1})	12.9	18.0	71.7	78.3
Bg (μT)	302	248	494.8	515.1

Table 4. NRM and GRM-related parameters for sample T1786 and T3470.

Sample	T1786	T3470
NRM (mA m^{-1})	4.82	1.02
GRM (mA m^{-1})	3.03	23.2
RRM (mA m^{-1})	341	439
ARM (mA m^{-1})	36	48
Bg (μT)	662	642.3

Table 5. Anisotropy of sample T1786 and T3470 based on GRM measurements along 6 different directions.[2]

	T1786			T3470		
	Int.	Dec.	Inc.	Int.	Dec.	Inc.
C1 ($y' - z'$)	32	74	18	241	241	−38
C2 ($z' - x'$)	−43	182	44	−280	320	14
C3 ($x' - y'$)	10.8	328	41	39	214	49

[2]Sample T3470, which acquired a GRM much higher than the NRM, has the higher anisotropy of both samples (see Stephenson 1981, 1993, for an explanation of such anisotropy results).

Table 6. Anisotropy data for sample T3470[3].

	Max		Int		Min	
	Dec.	Inc.	Dec.	Inc.	Dec.	Inc.
susc 1	39	39	308	1	217	51
susc 2	30	40	296	4	201	49
GRM 100	61	38	320	14	214	49
GRM 80	43	52	316	−3	228	38
RRM 80	90	22	346	31	209	51
ARM 80	110	10	14	32	216	56

[3]From measurements of magnetic susceptibility, GRM at 100 and 80 mT, and RRM and ARM at 80 mT.

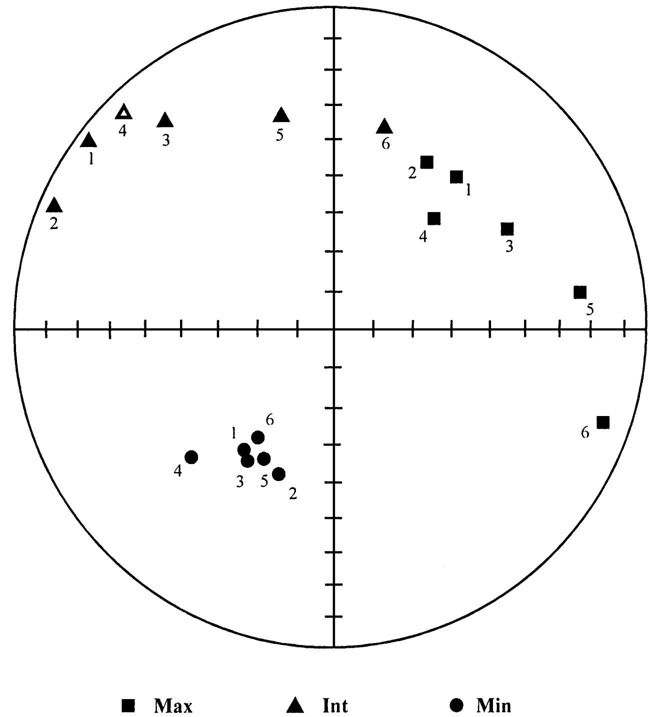

Figure 3. Distribution of anisotropy axes for magnetic susceptibility (denoted as 1 and 2, respectively), GRM imparted at 80 and 100 mT (denoted as 3 and 4, respectively), RRM and ARM at 80 mT (denoted as 5 and 6, respectively).

between z' and either x' or y' is much larger in sample T3470. This unequivocally demonstrates that sample T3470 has much higher anisotropy than sample T1786. From the B_g values, the mineralogy is presumably similar and so the higher anisotropy appears to be the reason why sample T3470 acquires a much higher GRM than sample T1786.

FURTHER ANISOTROPY MEASUREMENTS

As a further check on the anisotropy measurement of sample T3470 by the 6-axis GRM method using a peak AF of 80 mT, the anisotropy of RRM and ARM as described by Potter & Stephenson (1986) was also determined at the same peak AF together with a further 6-axis GRM measurement using a peak AF of 100 mT to check for consistency between results. The anisotropy of initial susceptibility was also measured for comparison. This was not done for sample T1786 because it was so much more weak than sample T3470. The results are summarised in Table 6 and Fig. 3. The anisotropy of magnetic susceptibility was measured twice with similar results. Anisotropies of GRM imparted with peak AFs of 80 and 100 mT are also similar. It can be seen from Fig. 3 that the axis with declination of 210° and inclination of 50° is detected as a minimum axis by all methods. The other two axes are, however, spread out over a great circle. This indicates that the ellipsoid is oblate, because there is not much difference between the intensities of these two axes, and thus they are not well defined. It is clear that the anisotropy of GRM and RRM is in consistent with that of susceptibility (as well as ARM). The use of 6 orientations to obtain anisotropy information from GRM measurements (Stephenson 1993) is relatively quick and is thus far more practical than more tedious methods used by Hu *et al.* (1998) and the earlier method of Stephenson (1981), and even is useful when paramagnetic and diamagnetic contribution to susceptibility is predominant.

CONCLUSIONS

Greigite from the Zoigê Basin, like other greigite-bearing samples, acquires large gyroremanences and has large values of the gyrofield (B_g) up to 734 μT. Because of this large gyromagnetic effect, it is difficult to correct for the acquisition of GRM when carrying out static 3-axis AF demagnetisation of the NRM because the GRM becomes more than an order of magnitude higher than the remaining NRM when the peak field starts to exceed 50 mT. Although GRM is a nuisance when attempting to carry out AF demagnetisation, it can be used to measure the increase in anisotropy of greigite-bearing sediments with depth (due to increased compaction) where susceptibility methods may not be sensitive enough (especially at shallow depth), or paramagnetic and diamagnetic contribution is significant. GRM can also be used to estimate the orientation of the anisotropy ellipsoid of greigite-bearing sediments at different depths. RRM (B_g value) measurements indicate that the magnetic mineralogy of the greigite-bearing sediments is similar, independent of depth.

ACKNOWLEDGMENTS

This work was funded by National Natural Science Foundation of China (grant Nr 40172102, 49872058) and Deutsche Forschungsgemeinschaft (grant AP 34/10-1).

REFERENCES

Dankers, P.H.M. & Zijderveld, J.D.A., 1981. Alternating field demagnetisation of rocks, and the problem of gyromagnetic remanence, *Earth planet. Sci. Lett.,* **53,** 89–92.

Dekkers, M.J. & Schoonen, M.A.A., 1996. Magnetic properties of hydrothermally synthesized greigite (F3S4); I, Rock magnetic parameters at room temperature, *Geophys. J. Int.,* **126,** 360–368.

Edwards, J., 1982. Gyroremanent magnetisation produced by specimen rotation between successive alternating field treatments, *Geophys. J. R. astr. Soc.,* **71,** 199–214.

Hallam, D.F. & Maher, B.A., 1994. A record of reversed polarity carried by the iron sulphide greigite in British early Pleistocene sediments, *Earth planet. Sci. Lett.,* **121,** 71–80.

Hoffmann, V., 1992. Greigite (Fe_3S_4): magnetic properties and first domain observations, *Phys. Earth planet. Inter.,* **70,** 288–301.

Hu, S., 1998. A magnetic study on lacustrine sediments from Zoigê Basin, Eastern Tibetan Plateau, China, *PhD thesis,* Universität Tübingen, Tübingen, Germany.

Hu, S., Appel, E., Hoffmann, V., Schmahl, W. & Wang, S., 1998. Gyromagnetic remanence acquired by greigite (Fe_3S_4) during static three-axis alternating field demagnetisation, *Geophys. J. Int.,* **134,** 831–842.

Hu, S., Appel, E. & Wang, S., 1999. A magnetic study on lacustrine sediments from Zoigê Basin, Eastern Tibetan Plateau, China: Magnetostratigraphy and environmental implications, *Physics and Chemistry of the Earth,* **24,** 811–816.

Mahon, S.W. & Stephenson, A., 1997. Rotational remanent magnetisation (RRM) and its high temporal and thermal stability, *Geophys. J. Int.,* **130,** 383–389.

Potter, D.K. & Stephenson, A., 1986. The detection of fine particles of magnetite using anhysteretic and rotational remanent magnetisations, *Geophys. J. R. astr. Soc.,* **87,** 569–582.

Roberts, A.P., 1995. Magnetic properties of sedimentary greigite (Fe_3S_4), *Earth planet. Sci. Lett.,* **134,** 227–236.

Roberts, A.P., Reynolds, R.L., Verosub, K.L. & Adam, D.P., 1996. Environmental magnetic implications of greigite (Fe_3S_4) formation in a 3 m.y. lake sediment record from Butte Valley, Northern California, *Geophys. Res. Lett.,* **23,** 2859–2862.

Roperch, P. & Taylor, K., 1986. The importance of gyromagnetic remanence in alternating field demagnetisation: some new data and experiments on GRM and RRM, *Geophys. J. R. astr. Soc.,* **87,** 949–965.

Sagnotti, L. & Winkler, A., 1999. Rock magnetism and palaeomagnetism of greigite-bearing mudstones in the Italian peninsula, *Earth planet. Sci. Lett.,* **165,** 67–80.

Smith, G. & Merrill, R.T., 1980. The origin of rotational remanent magnetization, *Geophys. J. R. astr. Soc.,* **64,** 329–336.

Snowball, I., 1991. Magnetic hysteresis properties of greigite (Fe_3S_4) and a new occurrence in Holocene sediments from Swedish Lappland, *Phys. Earth planet. Inter.,* **68,** 32–40.

Snowball, I., 1997a. Gyroremanent magnetisation and the magnetic properties of greigite-bearing clays in southern Sweden, *Geophys. J. Int.,* **129,** 624–636.

Snowball, I., 1997b. The detection of single-domain greigite (Fe_3S_4) using rotational remanent magnetisation (RRM) and the effective gyro field (B_gBg): mineral magnetic and paleopalaeomagnetic applications, *Geophys. J. Int.,* **130,** 704–716.

Stephenson, A. & Snowball, I., 2001. A large gyromagnetic effect in greigite, *Geophys. J. Int.,* **145,** 570–575.

Stephenson, A., 1980b. A gyroremanent magnetisation in anisotropic magnetic material, *Nature,* **284,** 49–51.

Stephenson, A., 1981. Gyromagnetic remanence in single-domain particles, rocks, and magnetic recording tape, *Phil. Mag.,*B **44,** 635–664.

Stephenson, A., 1988. Gyroremanent magnetisation in self-reversing lithium chromium ferrite, *Phil. Mag.,* **58,** 91–102.

Stephenson, A., 1993. Three-aAxis static alternating field demagnetisation of rocks and the identification of natural remanent magnetisation, gyroremanent magnetisation, and anisotropy, *J. geophys. Res.,* **98,** 373–381.

Stephenson, A. & Molyneux, L., 1987. The rapid determination of rotational remanent magnetisation and the effective field which produces it, *Geophys. J. R. astr. Soc.,* **90,** 467–471.

Stephenson, A., 1980a. Gyromagnetism and the remanence acquired by a rotating rock in an alternating field, *Nature,* **284,** 48–49.

Torri, M., Fukuma, K., Horng, C.S. & Lee, T.Q., 1996. Magnetic discrimination of pyrrhotite- and greigite-bearing sediment samples, *Geophys. Res. Lett.,* **23,** 1813–1816.

Wilson, R.L. & Lomax, R., 1972. Magnetic remanence related to slow rotation of ferromagnetic material in alternating magnetic field, *Geophys. J. R. astr. Soc.,* **30,** 295–303.